Classification
Physics Abstracts
61.30 — 64.70 — 62.20D

Freeze-fracture observations in the L_α phase of a swollen surfactant in the vicinity of the L_3 and the L_1 phase transitions

P. Boltenhagen ([1], *), M. Kleman ([2]) and O. D. Lavrentovich ([3])

([1]) Laboratoire de Physique des Solides, Bât. 510, Université de Paris-Sud, 91405 Orsay Cedex, France
([2]) Laboratoire de Minéralogie-Cristallographie, Universités Pierre et Marie Curie (Paris VI) et Paris VII, 4 place Jussieu, case 115, 75252 Paris Cedex 5, France
([3]) Kent State University, Liquid Crystal Institute, Kent, Ohio, 44242, U.S.A.

(*Received 2 July 1993, revised 13 April 1994, accepted 18 April 1994*)

Abstract. — Freeze-fractured specimens of the L_α phase of a swollen quasi-ternary surfactant (cetylpyridinium chloride/hexanol/brine), have been observed by electron microscopy. The textures show the same features as those oberved by optical microscopy, viz. defects with negative Gaussian curvature (focal conic domains of the usual type) close to the phase boundary with the L_3 sponge phase, and defects with positive Gaussian curvature (focal conic domains of second species, mostly spherolites) close to the phase boundary with the L_1 micellar phase. We have studied in more detail this latter region : the density of spherolites increases as one approaches the L_1-L_α transition, up to the point where they seemingly fill the whole space ; their size distribution obeys an exponential law we explain by a simple thermodynamic model which predicts a transition when the elastic coefficient $\Lambda = 2K + \bar{K}$ vanishes. Our experimental data yield indeed, with a reasonable precision, a very small value of $\Lambda d/k_B T$ for a composition of the surfactant close to the phase boundary.

1. Inroduction.

Swollen lamellar phases (L_α) constituted by equidistant bilayers of amphiphilic molecules separated by water have been extensively studied for their structural properties [1], their stability with respect to their neighbouring phases in the phase diagram [2], their defects [3, 4]. Regarding this last point, it should be noted that these defects have been first observed at large scales by optical microscopy [3, 4], but very little is known at microscopic scale. This paper reports on electron microscopy observations of freeze-fractured specimens which have been prepared by the standard method : a small drop of the L_α phase is inserted between two copper plates and quenched into liquid propane, then fractured in vacuum ; a thin film of carbon-

(*) *Permanent address* : Institut de Physique, 3 rue de l'Université, 67084 Strasbourg Cedex, France.

platinum is evaporated on the fracture, detached from the sample, and finally observed (for details on this technique, see for example Ref. [5]). These observations confirm the results obtained at larger scales, implying that the defects are of the same nature at all scales, and bring some new results which are of a particular interest near phase transitions. Amongst those, the lamellar-micellar (L_1-L_α) transition is studied in more detail ; the defects appear to be thermodynamically stable, and the quantitative study of their distribution in size allows one to determine the values of the rigidity moduli of the layers.

We have investigated the L_α phase of the quasi-ternary system cetylpyridinium chloride (noted CpCl)/hexanol/brine (1 % by weight of NaCl). This lamellar phase extends in the phase diagram (see Ref. [1]) between a micellar (L_1) phase for low hexanol *versus* CpCl ratio ($r = h/c \sim 0.5$) and a sponge (L_3) phase for $r \sim 1$. Let us briefly recall the results obtained by optical microscopy observations.

In the vicinity of the L_α-L_3 phase transition, the typical observed defects layers are the well-known focal conic domains of the first species (FCD-I), characterized by constant layer thickness and negative Gaussian curvature of the layers i.e. $\sigma_1 \sigma_2 < 0$. On the contrary, in the vicinity of the L_α-L_1 phase transition, the defects have positive Gaussian curvature $\sigma_1 \sigma_2 > 0$; most of them are spherolites, that are degenerate focal conic domains of the second species (noted hereunder FCD-II), with a few FCD-II's of a more generic nature (for details see Ref. [4]). The differences between the defects representative of the two regions of the phase diagram close to the phase limits can be traced to a difference in the sign of the saddle-splay elastic constant $\bar{K}$ which governs the Gaussian curvature (Fig. 1) ; a quantitative analysis of the results has yielded an estimation of the values of this material parameter [3, 4].

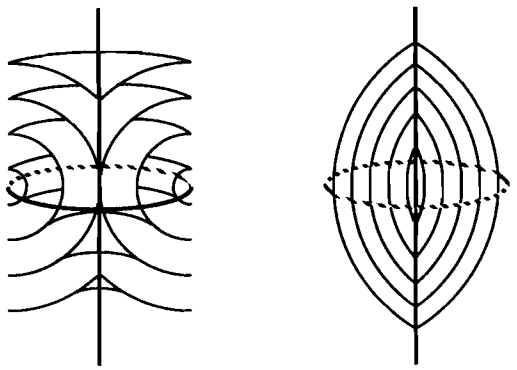

Fig. 1. — Focal conic domains, degenerate cases : a) FCD-In $\sigma_1 \sigma_2 < 0$; FCD-II, $\sigma_1 \sigma_2 > 0$. The circle is virtual in the case of FCD-II.

2. Energy density of a lamellar phase.

This section summarizes a few well-known aspects of the phenomenological description of lamellar phases and of their defects which are of importance in the following discussion.

The energy density of a lamellar phase reads, to quadratic order :

$$f = 1/2\, K(\sigma_1 + \sigma_2)^2 + \bar{K}\sigma_1 \sigma_2 + 1/2\, B\varepsilon^2 . \quad (1)$$

In this expression σ_1 and σ_2 are the principal curvatures of the bilayers, ε is the relative variation of the layers thickness, K and $\bar{K}$ are the splay and saddle-splay elastic constants, and B is the compressibility modulus [6].

Equation (1) contains three terms.

The first two are related to the mean curvature $\sigma_1 + \sigma_2$ and the Gaussian curvature $\sigma_1 \sigma_2$ of the bilayers, respectively. The second term is generally omitted because it does not enter in the minimization of the energy. This is a direct consequence of the Gauss-Bonnet theorem which states that the integral of the Gaussian curvature over a closed surface depends only on its topology :

$$\int \sigma_1 \sigma_2 \, d\Sigma = 4 \pi (1 - N) \tag{2}$$

(N is the number of handles on the surface). For example the integral of equation (2) is equal to 0 for a torus and to 4π for a sphere. Thus this term is a constant and can be neglected in any smooth continuous deformation of the system ; however it plays an important role in any change in the topology of the layers.

A complete description of the energy of the system requires to take into account the energy of interaction between the bilayers. This is the third term of equation (1). For an electrically neutral system, as it is the case here, this term is of entropic nature and has been studied by Helfrich [7].

Focal conic domains (FCD) are the typical defects of lamellar phases. Their characteristics can be simply inferred from equation (1). The energies associated with a pure curvature deformation or with a pure compression deformation at large scales (larger than a typical layer periodicity) are very different in magnitude, telling us that the system will choose to deform in a set of a quasi-equidistant and parallel surfaces, i.e. with vanishingly small compression energy. It can be shown that, if so, the system forms FCD's, in which the layers take the shape of Dupin cyclides [8].

Let us recall the basic features of a FCD. In each domain the layers are folded around two conjugate focal lines, viz. an ellipse and a hyperbola, in such a way that everywhere they are perpendicular to the straight lines joining any point E on the ellipse to any point H on the hyperbola. If the actual part of the layers is between E and H, $\sigma_1 \sigma_2 < 0$; in the opposite situation $\sigma_1 \sigma_2 > 0$. These are the defects observed at optical scales. Figure 1 illustrates the cases where the ellipse is degenerate to a circle and the hyperbola to a straight line, and illustrates the differences between a FCD-I ($\sigma_1 \sigma_2 < 0$) and a FCD-II ($\sigma_1 \sigma_2 > 0$). The reader will easily recognize that the two cases do not correspond to two different realizations of a FCD built on the same focal lines.

3. Results.

Starting from the vicinity of the L_1-L_α phase transition, a first remarkable result is that the lamellar phase is filled with spherolites whose density depends critically on the h/c ratio (Fig. 2). In each spherolite the lamellae form concentric spheres. The spherolites are polydisperse in size and their size distribution follows some characteristic exponential law which repeats remarkably well from one part of the sample to another (Fig. 3). At first sight, the whole space seems to be filled by spherolites of different sizes, but a closer look at the pictures reveals the presence of the layered matrix in a reasonable proportion indeed. An estimate of this proportion (made farther on) shows that the planar matrix fills approximately half the volume of the sample. The presence of this large matrix of well-oriented L_α phase suggests also that the fracture which is performed at low temperature in the freeze-

Fig. 2. — Freeze-fractured specimen, electron microscopy observation : spherolites near the L_1-L_α phase transition. The lamellar phase is filled with polydisperse spherolites. Note the presence of elongated FCD-II (arrow). hex/CpCl = 0.7 ; 85 % solvent. Bar 5 μm.

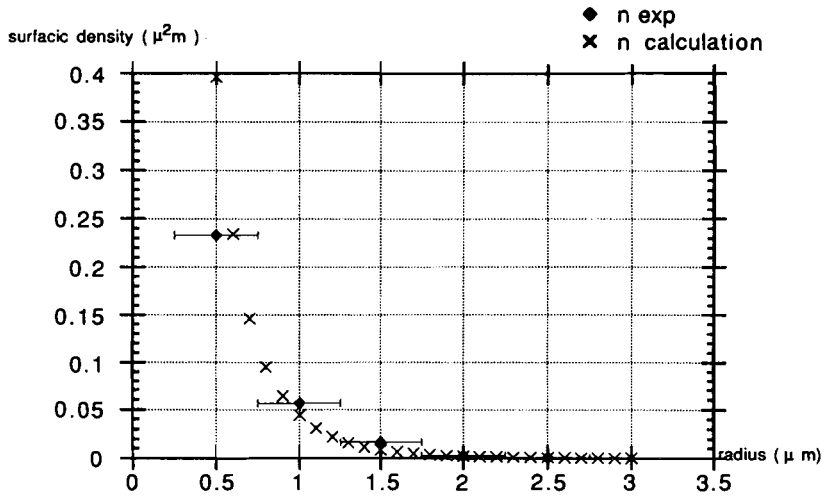

Fig. 3. — Hodograph of the surface density of spherolites as a function of the radius measured in freeze-fractured specimens. The horizontal error bar (ΔR) is the experimental error of measurement of the radii. The density error (Δn) is not represented, it is equal to $\Delta n = \frac{\delta n}{\delta R} \Delta R$.

fracture experiment, and which is well-known to easily follow the layers in such a type of material, is practically planar. The typical size of the spherolites which are observed is about one micrometer. Note the presence of generic FCD-II's, which are not perfectly spherical « spherolites », but have the shape of rugby balls. It has been shown elsewhere [3b, 4] that spherolites are the FCD-II's of smallest energy, for a given volume.

The increase of the hexanol *versus* CpCl ratio $r = h/c$ leads to a progressive disappearance of the spherolites. In the middle of the lamellar phase, for h/c between the L_1-L_α and L_α-L_3 phase transitions, we observe isolated spherolites embedded in the lamellar phase (Fig. 4). These observations confirm the large scales results.

In the vicinity of the L_α-L_3 phase transition the lamellae are very distorted (Fig. 4). A number of them are in contact along areas whose typical size is of the order of one micrometer : we do not know whether these contacts are dynamic or static, but they clearly announce the formation of the numerous pores which are present in the L_3 phase. Furthermore we observe a large number of screw dislocations, whose stability is most probably related to the negative Gaussian geometry of their cores [6]. Note that the areas which surround the zones of contact between lamellae are often of negative Gaussian curvature.

4. A simple model for spherolites.

We restrict here our discussion to the most novel aspect of this work, viz. the formation of a thermodynamically stable set of spherolites, whose density decreases when h/c increases, near the L_α-L_1 phase transition. This part is theoretical. The comparison with density measurements is made in the next section.

Let R be the diameter of a perfect spherolite ; according to equation (1) its total curvature energy writes :

$$W_C(R) = 4\,\pi \int_0^R f(r)\, r^2\, dr = 4\,\pi\,(2\,K + \bar{K})\,R\,. \tag{3}$$

To this energy should be added two terms. The first one, W_D, relates to the disclination loop which circles the spherolites at the contact with the outer layers (Fig. 1b) ; this energy scales like the perimeter and is of the order of KR. The second one, W_B, is due to the layer compressibility ; as shown in reference [3b], it scales like $B\lambda R^2$ with $\lambda = (K/B)^{1/2}$ for spherolites whose mean distance δ is larger than R^2/λ, (R^2/λ is the distance on which the stresses decrease exponentially [9]. But, if $R \leqslant \delta \leqslant R^2/\lambda$, a different model should be used ; we believe indeed that the stresses are relaxed by the presence of dislocation loops of size comparable to δ, so that W_B scales as a core energy $K\delta \approx B\lambda^2\delta$. We shall check that $\delta \approx R$, so that $W_B \approx B\lambda^2 R$. Furthermore, the situation we have investigated is close to the L_1 phase, where B is small, so that this term should not be very relevant. Putting together these results, we have :

$$W_{tot} = 4\,\pi\,\Lambda'\,R \tag{4}$$

where Λ' is a renormalized value of the quantity $\Lambda = 2\,K + \bar{K}$.

We assume that the free energy density F is a sum of independent terms $\sum_R F_R + F_0$. Each F_R refers to the set of spherolites of radius $R \neq 0$, and F_0 refers to the part of the sample which is not in a « spherolitic » state. We shall also use a continuous version of F, viz. $F = \int F_R \frac{dR}{d} + F_0$, where d is the repeat distance of the L_α phase. The volume density of

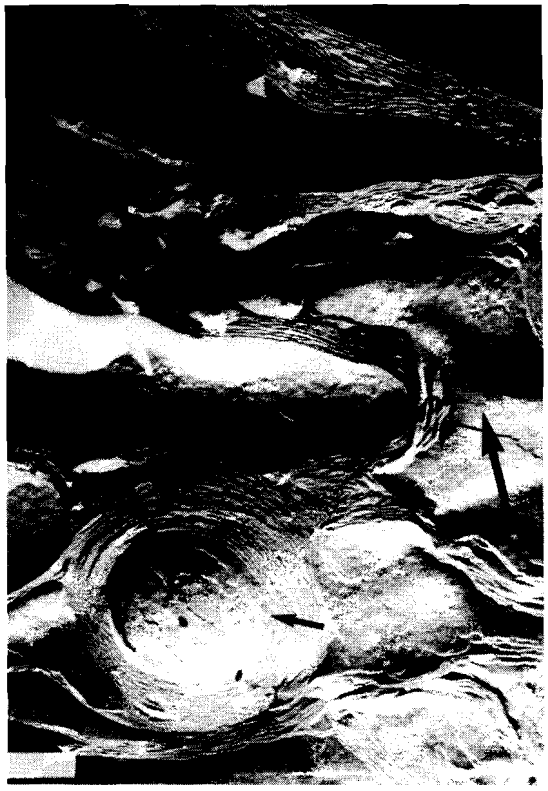

Fig. 4. — Freeze-fractured specimen, electron microscopy observation : in the middle of the L_α phase. Note the presence of spherolite embedded in the lamellar phase. The lamellar phase shows positive Gaussian curvature (small arrow) as well as negative Gaussian curvature (big arrow). hex/CpCl = 0.8 ; 85 % solvent. Bar 0.5 μm.

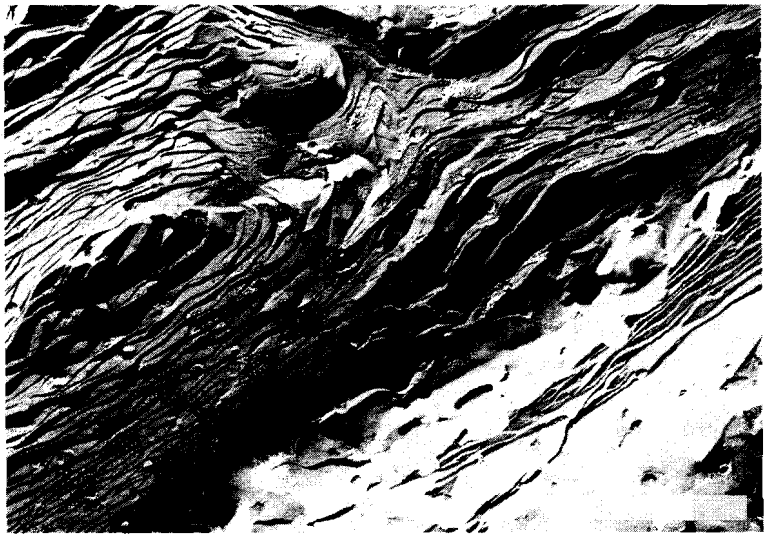

Fig. 5. — Freeze-fractured specimen, electron microscopy observation : aspects of the membranes near the L_α-L_3 phase transition. Note the numerous pores in formation. hex/CpCl = 1.0 ; 85 % solvent. Bar 0.5 μm.

spherolites of radius R is noted $n_R = \phi_R/v_R$, where ϕ_R is the volume fraction, and $v_R = 4\ \pi R^3/3$. We have :

$$F_R = \frac{1}{v_R} [4\ \pi \Lambda' R\phi_R + k_B T\phi_R \ln \phi_R] \tag{5}$$

where $\phi = \sum_R \phi_R$. The estimation of F_0 is a real difficulty in the present problem. In fact, while the *structure* of the free energy density F_0 remains unknown, its *variation* can be reached more easily. *It would be wrong to write :* $F_0 = \frac{1}{v_0} k_B T(1 - \phi) \ln (1 - \phi)$ where v_0 is some mean volume of an « elementary object » relative to the « non spherolitic » part of the sample. The molecules themselves, being so small compared to the spherolites, do not know whether they belong or not to a spherolite ; hence they play no rôle in the total balance of the entropy when a variation $\delta\phi_R$ occurs, except may be along the singularities (the equators of the spherolites and their centers), but this contribution scales like the entropy of the spherolites themselves and does not bring anything new. The molecules are not these elementary objects. On the other hand, the variation of the density of the spherolites strongly affects the entropy of the non-spherolitic part. Consider a variation $\delta\phi = \delta\phi_R$, i.e. restricted to some particular value of R. This variation affects F_R, but also F_0, since ϕ varies. The quantity :

$$S_R = \frac{k}{v_R} (1 - \phi) \ln (1 - \phi) \tag{6}$$

would be the entropy of the non-spherolitic part supposed filled (in a gedanke experiment) with non-spherolites of size R. The reasoning follows in fact closely the approach used to calculate the entropy of vacancies in a *monoatomic* crystal. This means also that the appearance (or conversely, the disappearance) of some relative volume $\delta\phi_R$ of spherolites of radius R involves a relative number of « elementary objects » $\delta\phi_R/v_R$. Hence the variation of the entropy of the non-spherolitic part would be $\delta S_R = \frac{k}{v_R} \delta\phi_R \ln e(1 - \phi)$, and the variation of the total free energy F_0, which is the sum of the entropy variations should therefore read :

$$\delta F_0 = - k_B T \sum_R \frac{\delta\phi_R}{v_R} \ln e(1 - \phi) . \tag{7}$$

In the continuous version, we replace $\sum_R \phi_R$ by $\int \phi_R \frac{dR}{d}$ and equation (7) by

$$\delta F_0 = - k_B T \int_0^\infty \frac{\delta\phi_R}{v_R} \ln e(1 - \phi) \frac{dR}{d} .$$

Entropy has been taken into account in equations (5) and (7) with the assumption that the spherolites form a regular solution of species labelled by the different values of R. This mean-field picture overestimates the total entropy and the total internal energy, since it neglects all correlations between spherolites of different sizes. The latter assumption might however be valid to a large extent. As indicated above, the interaction is mostly of elastic origin (B term). Consider then two sets of spherolites R_0 and R_1 ; they form two distinct *disordered* nets with *uncorrelated* characteristic distances δ_0 and δ_1 ; hence the energy of interaction of the two nets does not depend on the small fluctuations of their individual spherolites, nor on the relative « phase » of the two nets. Therefore we expect that the *long-range* elastic interactions

are mostly intra-net. *Short-range* interactions, i.e. those related to the excluded volume effects between spherolites belonging to different nets, will be neglected. Note further that the B term becomes probably less important near the L_α-L_1 phase transition, a fact which decreases even more the elastic interaction and eventually brings Λ' closer to Λ. Let us now examine the free energy in more detail ; we distinguish two cases :

i) $\Lambda' > 0$. Minimizing F with respect to ϕ_R yields :

$$\phi_R = (1 - \phi) \exp\left[- \frac{4\,\pi \Lambda' R}{k_B T} \right]. \tag{8}$$

When integrating this expression with respect to R, we get :

$$\phi = \frac{k_B T}{k_B T + 4\,\pi \Lambda' d}. \tag{9}$$

The inequality $(\partial^2 F/\partial \phi^2)_R > 0$ is satisfied, whatever R may be, when ϕ_R takes the value of equation (8) : the solution is stable. It can also easily be shown that, for the same value of ϕ_R, $(\partial F_R/\partial R)_{\phi_R}$ cannot vanish. Hence it is not possible to minimize the free energy with respect to R and there is no unique solution for R : we expect a *distribution* of spherolites of different sizes. One can finally show that the appearance of these defects in the L_α phase decreases the free energy of the perfectly flat phase.

According to equation (9), the medium is entirely invaded by the spherolites (i.e. $\phi \to 1$), when $\Lambda' \to 0$. This implies that the L_α phase with spherolites is no longer stable, and another phase does appear. The present approach does not enable us to define it any better. It is probably the L_1 phase.

ii) $\Lambda' < 0$. The same equations as above (Eqs. (8, 9)) still hold, but now equation (8) yields $\phi > 1$, which is inconsistent with the definition of ϕ. Therefore equation (7) does not describe properly the case $\Lambda' < 0$ (the L_1 phase ?).

5. Density measurements.

The theory developed for the case $\Lambda' > 0$ seems to describe reasonably well our experimental findings. The volume density n_R is related to the surface density n_R^s, i.e. the density measured experimentally in a 2D cut, by the relation $n_R^s = n_R^{2/3}$, which is easily obtained if one notices that $n_R^s\, \delta_R^{-1} = n_R$. Here $\delta_R^{-1} = n_R^{-1/3}$ is the mean distance between two spherolites of radius R. We can safely use this estimates of n_R, because the fracture is quasiplanar, as argued above. Comparison of equation (8) with experimental data (Fig. 3) yields the following expression for n_R^s :

$$n_R^s = \left[(1 - \phi) \frac{3}{4\,\pi R^3} \right]^{2/3} \exp\left(- \frac{2}{3} 3.6 \times 10^{-2} \frac{R}{d} \right) \tag{10}$$

where 3.6×10^{-2} is the slope of the logarithmic plot of $n_R^s R^2$ as a function of R/d. The corresponding value of ϕ obtained from equation (9) is 0.56, while the experimental value obtained from the plot of figure 3 is 0.52.

Since this expression yields so small a value for Λ', we assume $\Lambda' \sim \Lambda$ and get $\bar{K}/K$ as :

$$\frac{\bar{K}}{K} = -2 + 3.6 \times 10^{-2} \frac{k_B T}{4\,\pi k_c} \tag{11}$$

where $k_c = Kd$.

The periodicity d of the lamellar phase studied here is typically of the order of 150 Å ; the curvature modulus of the lamellar phase is about a few $k_B T$, thus

$$\eta = + 3.6 \times 10^{-2} k_B T/4 \pi k_c$$

is small and positive.

We found that $\bar{K}/K$ is very close to the value at which $\Lambda \to 0$, where we expect a divergence of the volume fraction of defects, i.e. a phase transition.

If $\Lambda = 2K + \bar{K}$ is small, the phase must be filled with spherolites, which is the case when h/c is small. A contrario when Λ increases the phase should have a lower density of spherolites. Experimentally we found that this is the case. Thus the increase of h/c leads to an increase of $\bar{K}/K$.

6. Why the distribution is not fractal.

We end this discussion by a brief comment on the fact that the distribution is exponential, *not* algebraic, i.e. not fractal.

Let us first recall that a fractal distribution has already been invoked in the problem of filling space with (conically shaped) FCD-I's [10]. There are similarities, but also differences between the two problems. In particular, while the filling with spheres is a genuine 3D problem, the FCD-I space filling is 2D : the length of the cone is equal approximately to the characteristic size L of the sample, while the base has a radius a which ranges from $\sim L$ to some small value a^*. According to reference [10], one first places inside the sample the largest possible domain, with base radius $a \sim L$, then the gaps are filled with smaller domains, in such a way that neighboring domains are in contact along a generatrix of the cones (Friedel's law of corresponding cones [8]) and the bases are tangent. This process continues down to molecular scales, with $a^* \sim \lambda \sim \sqrt{K/B}$. The result $a^* \sim \lambda$ is an intrinsic feature of the model, since the space filling is the result of a competition between layer compressibility and curvature elasticity. However, there is another natural limit for a^* in the FCD-I filling, which originates in the anisotropy $\Delta\sigma$ of the surface tension. As a matter of fact, the part of the sample which does not belong to a FCD-I can be either filled with FCD-II (at least in certain geometries [11]), or by dislocation loops which relax the layer elasticity. The regions with FCD-I and FCD-II fillings have different surface orientations ; as a result, the balance of the surface and curvature terms yield a new characteristic length [12], $a^* \sim K/(-\Delta\sigma)$ which can be very different from λ.

Let us now consider in turn the other type of space filling, with FCD-II's. There is only one characteristic length for each spherical FCD-II, viz. its radius a (we restrict our considerations to spherolites), which varies from some macroscopic value L (in general the sample size at rest ; a length depending on the shear rate, if any, has been introduced in Ref. [13]) to some minimal a^*. There are no special geometrical conditions akin to Friedel's law of corresponding cones when two spherolites are neighbors (there is no way to eliminate the elastic distortion of the layers) as in the FCD-I case, and there is no anisotropy of the global geometry, which is 3D, consequently we do not expect special surface tension effect which would specify a^*.

Having pointed out these differences with FCD-I's *iterative filling*, let us now put the stress on the differences with the former *exponential filling*. A fractal of spheres of different sizes would be inhomogeneous at all scales, so that our previous arguments about the irrelevance of the elastic interactions would fail ([1]). Assuming that the spheres pack randomly, the elastic

([1]) Reciprocally, we may wonder whether the growth process of a set of objects into the shape of a fractal is not due to a strongly inhomogeneous distribution of stresses which do not relax during growth.

energy now probably scales like the residual volume [10]. Let $g = (L/r)^{\gamma}$ be the numbers of spheres of radius R larger than r packed in a volume $\Omega \approx L^3$. The residual volume is $V(r) = \Omega (L/r)^{\gamma - 3}$; the total free energy $F(r)$ scales like :

$$F(r) \cong A\Omega (L/r)^{\gamma - 1} + B\Omega (L/r)^{\gamma - 3} . \quad (12)$$

There is no entropy term, because the packing processes which starts from the biggest spheres ($R \approx L$), in a volume of size L, continues with spheres of decreasing sizes, is pratically deterministic (but to indiscernability of equal spheres). The smaller the residual volume, the more so. According to reference [14], a relevant value of the exponent γ is ca. 2.8. This value yields indeed i) a minimum of $F(r)$ when $A > 0$ (the condition for a minimum to exist being $1 < \gamma < 3$) and ii) a minimum value for r, viz. : $r_{\min} \cong \sqrt{A/B}\ (\gamma - 1)/(3 - \gamma)$. The latter minimum does not show up in the former theory ; furthermore the energy is now positive. In other words, a fractal random packing cannot describe a phase with thermodynamic defects, but a possible phase of another nature.

Acknowledgments.

O. Lavrentovitch thanks the Laboratoire de Physique des Solides (Orsay) and the NSF (grant DMR89-20147 ALCOM) for support.

References

[1] Gomati R., Appell J., Bassereau P., Marignan J. and Porte G., *J. Phys. Chem.* **91** (1987) 6203.
[2] Porte G., Appell J., Bassereau P. and Marignan J., *J. Phys. France* **50** (1987) 1339.
[3] Boltenhagen P., Lavrentovich O. and Kleman M., a) *J. Phys. II France* **1** (1991) 1233 ; b) *Phys. Rev. A* **46** (1992) R1743.
[4] Boltenhagen P., Kleman M. and Lavrentovich O., *C.R. Acad. Sci. Paris* **315** (1992) 931.
[5] Freeze Fracture : Methods, Artifacts and Interpretations, J. Rash and S. Hudson Eds. (Raven Press, N.Y., 1981).
[6] Kleman M., Points, Lines and Walls, chapt. 5 (Wiley & Sons, 1983).
[7] Helfrich W., *Z. Naturforsch.* **33a** (1978) 305.
[8] Friedel G., *Ann. Phys. Paris* **2** (1922) 273.
[9] Durand G., *C.R. Acad. Sci. Paris* **275B** (1972) 629.
[10] Bidaux R., Boccara N., Sarma G., de Sèze L., Parodi L. and de Gennes P. G., *J. Phys. France* **34** (1973) 661.
[11] Sethna J. P. and Kleman M., *Phys. Rev. A* **26** (1982) 3037.
[12] Lavrentovich O. D., *Sov. Phys. JETP* **64** (1986) 984.
[13] Diat O. and Roux D., *J. Phys. II France* **3** (1993) 9.
[14] Omnès R., *J. Phys. France* **46** (1985) 139.